Hydrol. Earth Syst. Sci. Discuss., 11, 11395–11438, 2014
www.hydrol-earth-syst-sci-discuss.net/11/11395/2014/
doi:10.5194/hessd-11-11395-2014

Hydrology and Earth System Sciences
Discussions
Open Access

Optimal well locations using genetic algorithm for Tushki Project, Western Desert, Egypt

S. Khalaf[1] and M. I. Gad[2]

[1]Irrigation and Hydraulics Dept., Faculty of Engineering, Mansoura University, Mansoura, Egypt
[2]Hydrology Division, Desert Research Center, Cairo, Egypt

Received: 5 September 2014 – Accepted: 30 September 2014 – Published: 15 October 2014

Correspondence to: S. Khalaf (samykhalaf2005@yahoo.com)

Published by Copernicus Publications on behalf of the European Geosciences Union.

Abstract

Groundwater depletion is one of the most important problems threaten the national projects in Egypt. The optimal distribution of well locations and pumping rates mitigate this problem. In this paper, a trial to mitigate this problem in Tushki National Project, south western desert, Egypt was carried out via delineating the optimal well locations and optimal pumping rates. The methodology of combination between simulation and optimization techniques was applied. A linked simulation-optimization model for obtaining the optimum management of groundwater flow is used in this research. MODFLOW packages are used to simulate the groundwater flow system. This model is integrated with an optimization model OLGA (**O**ptimal well **L**ocation using **G**enetic **A**lgorithm technique) which is based on the genetic algorithm (GA). Two management cases were considered by running the model in Abu Simbel-Tushki area with adopted steady and transit calibrated parameters. The first case (fixed well location) is found that the optimum value of the objective function (maximum pumping rate). In the second case (flexible well location with the moving well option) locations of wells are to be decided by the OLGA model itself within a user defined region of the model grid until the optimal location is reached. Also, the prediction of the future changes in both head and flow were made in steady and transient states.

1 Introduction

Groundwater sustainable planning and management strategy in under-developed regions of North Africa, the Middle East, South and Central Asia, North China, North America, and Australia and localized areas throughout the world is one of the most important issues. The groundwater resources in these areas had been deteriorating due to the absence of the optimal operation of groundwater system strategy. One of the best methods of determining the optimal operating strategy for a groundwater system may be the combined use of simulation/optimization (S/O) models. While simulation models

HESSD
11, 11395–11438, 2014

Optimal well locations using genetic algorithm for Tushki Project

S. Khalaf and M. I. Gad

basically provide solutions of the governing equations of groundwater flow, optimization models identify an optimal management and planning strategy from a set of feasible alternative strategies. The genetic algorithm (GA) was widely used to modify the parameters of groundwater flow models (Yan et al., 2003; Yao et al., 2003) and to solve the management models of groundwater resources (Mckinney and Lin, 1994; Liu et al., 2002; Zhu et al., 2003) because it has some virtues. The seminal work on GA was done by Holland (1975). The development and application of the coupled simulation optimization approach had been an active and fruitful research area in last years (Gorelick, 1983; Ahlfeld et al., 1988; Wanger and Gorelick, 1989; Gulver and Shoemaker, 1992; Rizzo and Dougherty, 1996). McKinney and Lin (1994) presented simulation optimization model based on GA to solve three groundwater management problems, maximum pumping from an aquifer, minimum cost water supply development, and minimum cost aquifer remediation. Rana et al. (2008) conducted a study on a spatio-temperal optimization of agricultural drainage, using groundwater model and GA. Guan et al. (2008) proposed an improved genetic algorithm (IGA) to solve optimization problems with equality and inequality constraints. Hamid et al. (2009) presented a paper focusing on the S/O for conjunctive use of surface water and groundwater on a basin-wide scale, the Najafabad plain in west-central Iran. Moharram et al. (2012) applied SOGA model (Single Optimization and Genetic Algorithm model) to predict the optimal pumping rate from El-Farafra depression. The results showed that the optimal pumping rate was 183 023 $m^3\,day^{-1}$ under the current situation of 48 productive wells. Gad et al. (2011) used a model of optimization based on the combination of the MODFLOW simulation with GA to maximize the total pumping rate from the Nubian sandstone aquifer in El-Dakhla depression at steady-state. The results showed that under the increasing of pumping rate by 25 %, the optimal pumping rate and drawdown ranged from 638 138 to 595 978 $m^3\,day^{-1}$ and from 4.29 to 10.36 m respectively. Saafan et al. (2011) applied multi-objective genetic algorithm (MOGA) model in El-Farafra oasis, Egypt to develop the maximum pumping rate and minimum operation cost as well as the prediction of the future changes in both pumping rate and pumping operation cost. They concluded

HESSD
11, 11395–11438, 2014

that the optimal pumping rate and the corresponding drawdown range from 190 699 to 179 423 $m^3 day^{-1}$ and 6.13 to 8.34 m respectively. Gad and Khalaf (2013) used MOGA model to develop the maximum pumping rate and minimum operation cost as well as to predict the future changes in both pumping rate and pumping operation cost in the Miocene aquifer of Wadi El-Farigh, West Delta, Egypt. They concluded that the compromise solution among the set of Pareto optimal solutions for the three proposed scenarios in MAIWF at year 2050 are optimal pumping of 576 130 $m^3 day^{-1}$ with optimal cost of USD 533 332 for the first scenario, optimal pumping of 667 130 $m^3 day^{-1}$ with optimal cost of USD 617 572 for the second scenario and optimal pumping of 596 212.7 $m^3 day^{-1}$ with optimal cost of USD 531 481 for the third scenario.

In the other side, there are limited studies for the determination of optimal operating strategy, including unknown well locations and pumping rates, for groundwater systems to the best of our knowledge (Wang and Ahlfeld, 1994; Karahan and Ayvaz, 2005; Ayvaz and Karahan, 2008). Saffi and Cheddadi (2007) developed an algebraic expression which gave the matrix of transient influence coefficients for a one-dimensional semi-confined aquifer model and solved the governing equation by using a mixed compartment model. They minimized the error between observed and simulated hydraulic heads to determine the illegal groundwater pumping at fixed well locations. Tung and Chou (2004) integrated pattern classification and tabu search to optimize the average zonal groundwater pumping for an aquifer. Their study also considered the minimization of the error between observed and simulated hydraulic heads. Research conducted in this field usually dealt with the identification of locations and released histories of unknown groundwater pollution sources (Mahar and Datta, 2000, 2001; Aral et al., 2001; Ruperti, 2002; Singh et al., 2004; Sun et al., 2006), pumping well optimization for optimum remediation design (Wang and Ahlfeld, 1994; Huang and Mayer, 1997; Guan and Aral, 1999; Zheng and Wang, 1999; Mantoglou and Kourakos, 2007; Chang et al., 2007), and optimum well locations and pumping rates in the coastal sides to prevent the saltwater intrusion problems (Cheng et al., 2000; Park and Aral, 2004; Ferreira da Silva and Haie, 2007). However, before performing these analyses, the locations and pumping rates of all the wells should be known since these wells may have a great impact in using S/O models.

The groundwater resources in the southern part of Western Desert of Egypt, **N**ubia **S**andstone **A**quifer of **T**ushki **A**rea (**NSATA**), are exposed to deteriorate due to the absence of the optimal operation of groundwater system strategy. This strategy is proposed, in this study, based on the **O**ptimal well **L**ocation using **G**enetic **A**lgorithm technique (**OLGA** model). This constructed model introduces a solution approach in which the locations and pumping rates of the productive wells are identified. Note that the optimization model used in this study determines the well configurations using genetic algorithm techniques while the simulation model solves the related problem for provided parameters of the optimization model.

1.1 Site description

Tushki area, is a part of the Western Desert of Egypt; between latitudes 22°14′24.75″ and 22°50′6.10″ N and longitudes 31°0′44.06″ and 31°50′4.05″ E, (Fig. 1). It has been subjected to some arid and wet periods in its past geologic history which reflect the present surface features. Tushki project, one of the national governmental and invest mental agricultural programs, aims to reclaim 540 000 acres using both surface water from Nasser lake (3 km^3 $year^{-1}$) and groundwater. The surface water was transported to the reclaimed areas by El-Sheikh Zayed Canal through its main channel (50 km) and four subsidiary branches. The surface water stands at level varying between +147 and +201 m near the huge Mubarak lifting station constructed at Lake Nasser. Moreover, another reclamation process is under execution in the area depending on groundwater of the NSATA which represents the main aquifer in the area. About 155 wells were already for this purpose (Fig. 1) besides 210 wells will be drilled by the end of the year 2017. All these activities are expected to have its effect on groundwater in the area. The main recharge of the NSATA depends upon the leakage from the Lake Nasser and/or the underground flow from the southwestern part. Due to the importance of the proper

HESSD
11, 11395–11438, 2014

productive wells locations for sustainability of the reclamation projects, this paper aims to demonstrate the optimal configuration of the productive wells using GA techniques.

1.2 Geomorphologic and geological settings

Referring to the geomorphologic map prepared by El-Shazly et al. (1980), CONOCO (1987), and Aggour et al. (2012) (Fig. 2) five geomorphologic units are distinguished in the study area. Nasser lake, the Nile valley, Wadi Kurkur pediplain, Tushki depression and West Dungul plain. Wadi Kurkur pediplain represents most parts of the area. The pediplain surface is covered mainly by nearly horizontal beds of Nubia sandstone, with outcrops of igneous and metamorphic rocks as well as several volcanic exposures. Few conspicuous hills in this part are also formed of relatively higher masses and ridges of Nubia sandstone capped by limestone beds representing remnants of younger sediments. Tushki depression area is an elongated featureless smooth plain covered to a great extent by sands with some soft clays and chalk. It is generally bounded by the topographic contour line of 200 m a.s.l. and is generally representing a topographic depression with an average absolute elevation of less than 200 m. It is bounded from the north and east by limestone plateau and from the south and the west by sandy pediplain and peneplain respectively.

Geologically, according to CONOCO (1987) (Fig. 2), the main geological units in Tushki area are the Precambrian Basement rocks and sedimentary succession. The basement rocks constitute some of the conspicuous ridges and high peaks in the area such as G. Umm Shaghir (+318 m), Stella ridge (+189 m) and G. El Asr (+264 m). The lithostratigraphic sedimentary succession in the study area is dominated by Cretaceous, Oligocene and Quaternary sediments (Fig. 2). The Lower Cretaceous rocks are differentiated into the Abu Simble, Lake Nasser and Sabaya formations. The Abu Simble Formation covers vast parts south of Khor Tushki with thickness ranges from 30 to 87.45 m (Aggour et al., 2012). It is composed mainly of a sequence of sandstone, ferruginous sandstone and siltstone beds with occasional conglomerate bands deposited under fluvial environmental conditions. The Lake Nasser Formation is underlain by the

HESSD
11, 11395–11438, 2014

Optimal well locations using genetic algorithm for Tushki Project

S. Khalaf and M. I. Gad

Abu Simble Formation and overlain by the Sabaya Formation. It is built up of ferruginous siltstone and ferruginous sandstone which reflects a coastal margin depositional environment. The lower part of Sabaya Formation consists mainly of sandstone while the upper one from finer grains sediments (siltstone) which reflects braided river conditions and sheet flows over channel banks for the lower and upper parts respectively. In addition, the Upper Cretaceous rocks are represented by Kiseiba Formation with 150 m thick. They are composed at its lower part of shale beds alternating with a few layer of siltstone, and the upper part with fossilferrous limestone, calcareous shale and marl. The Oligocene basalt rocks are widespread near the head of Khor Tushki, near G. El Sad and in the SW part of the study area where basalts are found as sheets overlying or interbedded with the Nubia Sandstone. Moreover, the Quaternary deposits are represented by sand accumulations and Alluvial sediments. The Alluvial sediments are deposited as a result of water floods along the shore of both Lake Nasser and the new Tushki lakes.

In additions, various structural elements are present among which are the uplift of the basement (Nakhlai-Aswan uplift trending NE–SW with 300 km long), E–W faults (north of Khor Tushki) and NW–SE faults (south of Khor Tushki), folds (sedimentary beds dip 15–45° forming limited basins and domes trending E–W and NE–SW), the Ring forms (Domes structure or basin forms) and the structural lineation (Fig. 3).

The structural density contour map (Fig. 3 left) reveals that the high density areas are defined by units B4, B5, C3 and E2 having values of 1.27, 1.21, 0.75 and 0.79 km^{-1} respectively. The unit areas A1, A2, A3, A4, A5, B1, B2, B3, C1 and C2 have low structural lineament density values of 0.53, 0.2, 0.29, 0.33, 0.34, 0.18, 0.21, 0.44, 0.31 and 0.38 km^{-1} respectively. These low densities are related to the area covered by shale and clay of the Tushki depression in which structural lineaments are not propagated to the surface (Aggour et al., 2012). Worth mention, these elements have proper impacts upon the groundwater occurrences. The fault systems play an important role in recharging the NSATA from Lake Nasser especially the NW–SE. They act as conduits

HESSD
11, 11395–11438, 2014

and help in transmitting the groundwater within the NSATA supporting the hydraulic connection between the aquifer units.

1.3 Hydrogeological aspects

The NSATA is mainly composed of porous and permeable ferruginous sandstone with clay intercalations forming three successive water-bearing units, namely; the Gilf, Abu Simble and Lake Nasser (south of Khor Tushki). The middle unit is an aquiclude that extends unbroken under the lake and leaks at periods longer than several years. The lower unit, overlying the granitic basement, is a confined aquifer of fluvial sandstones and has a large-scale (several kilometers). The groundwater of NSATA exists under unconfined (north of Khor Tushki) to semi-confined conditions depending on the occurrence, thickness, and continuity extent of the clay interbeds. The NSATA thickness decreases locally towards north and NW due to the presence of basement complex at shallow depths. The maximum thickness reaches 400 m. The transmissivity of the NSATA, as estimated from pumping tests (Fig. 3 right), increases from SW to NE which consistent with the direction of the structural lineaments density increase. Its estimated values range between 400 and 1900 $m^2 day^{-1}$ for the middle parts of Abu Simble and the northern part of Khor Tushki respectively. However, the high values of transmissivity coefficient in the northern part of Khor Tushki may attribute to the high sand percent (more than 70 %, Aggour et al., 2012) and high structural lineaments density which reflects an increase of the NSATA groundwater potentiality. In addition, the constructed equipotential contour maps (Fig. 4) show that the surface water level in Lake Nasser is generally higher than the groundwater level in the NSATA, as well as by the abrupt rise in groundwater level near the lake. The groundwater level in the NSATA indicates a local groundwater recharge from Nasser Lake to adjacent areas while the general groundwater flow is from SW to NE direction. This suggests the local recent recharge through the NW–SE and E–W faults (Korany et al., 2012). The groundwater flow rate was estimated as 0.044 $m day^{-1}$ (near Nasser Lake) and decreased to 0.044 $m day^{-1}$ towards northwestern parts (El-Sabri et al., 2010).

HESSD
11, 11395–11438, 2014

2 Material and methods

The materials used in this paper were collected through carrying out four field trips in Tushki area during the period 2010–2012. Two field trips were achieved with the team work of the Desert Research Center and the others for carrying out four pumping tests. The basic hydraulic parameters of NSATA are estimated based on both step and long duration pumping tests (Tables 1 and 2). The different hydrologic data are obtained during these field trips via the manager of irrigation sector office. In addition, two data loggers were installed by WRRI team work in the observation wells in the reclaimed areas and daily periodic records of the groundwater depth were measured during this work. These materials also include collection of archival data (well drilling reports, WRRI 2002), registration of discharge, distribution of wells, proposed operating systems for both groundwater supply and reclaimed area beside recording depth to water for groundwater level changes.

The methodological approach used in this paper is based on the mathematical modeling techniques which combines between simulation and optimization model. A computer programming with FORTRAN language has been originally established to apply the principles of the genetic algorithm for studying the optimal location of the groundwater productive wells as a principal tool for groundwater resources management. The Optimal well Location applying Genetic Algorithm (OLGA model) links MODFLOW with genetic algorithm technique to establish a simulation optimization groundwater model.

2.1 Simulation technique

Groundwater flow simulation is carried out applying MODFLOW software. MODFLOW simulates groundwater flow in aquifer systems using the finite-difference method. In this method, an aquifer system is divided into rectangular blocks by a grid. The grid of blocks is organized by rows, columns, and layers, and each block is commonly called a "cell". The model describes groundwater flow of constant density under non-equilibrium conditions in three-dimensional heterogeneous and anisotropic medium according to

HESSD
11, 11395–11438, 2014

the following equation (Bear, 1979):

$$\frac{\partial}{\partial x}\left(K_{xx}\frac{\partial h}{\partial x}\right)+\frac{\partial}{\partial y}\left(K_{yy}\frac{\partial h}{\partial y}\right)+\frac{\partial}{\partial z}\left(K_{zz}\frac{\partial h}{\partial z}\right)-W=S_{\mathrm{s}}\frac{\partial h}{\partial t} \tag{1}$$

in which; K_{xx}, K_{yy} and K_{zz} are values of hydraulic conductivity ($\mathrm{L\,T^{-l}}$); along the x, y, and z coordinate axes; h is the potentiometric head (L); W is the volumetric flux per unit volume and represents sources and/or sinks of water ($\mathrm{T^{-l}}$); S_{s} is the specific storage of the porous material ($\mathrm{L^{-1}}$); and t is time (T). The model was used the finite difference approach to solve the groundwater flow equation.

2.2 Conceptual model

On the light of the hydrogeologic properties of the NSATA, a pictorial representation (conceptual model) of the water flow system is constructed to this aquifer. The constructed conceptual model depends on the following facts (Kim and Sultan, 2002; DRC, 2012):

1. The basement surface forms an impervious lower boundary for the aquifer and acts as a barrier to the lateral groundwater flow in some locations. The lower part of the sequence consists of undifferentiated conglomerate, sandstone and shale.

2. The penetrated NSATA section is formed of fining downward litho-facies. The relatively high water level of Lake Nasser and the difference between its level and the groundwater level induce the water body of Lake Nasser to expose influent conditions (Aly et al., 1993). The groundwater flow direction in the NSATA south of Lake Nasser is from southwest to northeast, which means that it is following the general flow direction of the whole Nubia Sandstone aquifer in the western desert.

3. The NSATA groundwater occurs under the unconfined to semi-confined conditions.

HESSD
11, 11395–11438, 2014

S. Khalaf and M. I. Gad

2.3 Model Grid and boundary conditions

The model domain of NSATA is selected to cover 3315 km^2 (51 km × 65 km). The model domain is discretized using 130 rows × 102 columns rectangular cells. This discrimination produces 13 260 cells in the model layer. The width of the cells along rows (in *x* direction) is 500 m and along columns (in *y* direction) is 500 m. The grid geometry is shown in (Fig. 5). Moreover, depending on the groundwater flow pattern of the NSATA and the field measurements of the groundwater head in 68 wells of Abu Simbel-Tushki area, the initial and boundary conditions of the local model is defined. The water body of Lake Nasser is considered a time-constant head (fixed head-boundary condition) at level of 175 m a.m.s.l. (DRC, 2012). The equipotential contour line of 176 m a.s.l. characterizing to the SW corner is far enough from the well fields to be constant head boundary condition. The hydraulic heads and hydraulic conductance are assigned to boundary cells. These heads vary during the simulation process according to different stresses applied on the modeled area.

2.4 Model calibration

Model calibration entails changing values of model input parameters in an attempt to match field conditions within some acceptable criteria. Adjustment to model parameters, stresses, and boundaries will be limited within reasonable ranges that are based on available information. Model calibration requires that field conditions at a site be properly characterized. Lack of proper site characterization may result in a model calibrated to a set of conditions that are not representative of actual field conditions. The calibration process typically involves calibrating to steady-state and unsteady state conditions. With steady-state simulations, there are no observed changes in hydraulic head with time for the field conditions being modeled. Unsteady state simulations involve the change in hydraulic head with time (e.g. aquifer test, an aquifer stressed by a well field). Model calibration should include comparisons between simulated and observed heads. However, it is important that the modeler make every attempt to minimize the

HESSD
11, 11395–11438, 2014

difference between model simulations and measured field conditions. In the trial-and-error calibration process, the independent variables (parameters and fluxes) of a model are adjusted manually, in successive model runs, to produce the reasonable match between the simulated and measured data. Calibration of present model is carried out in two sequential stages, a steady state calibration followed by unsteady state calibration.

2.5 Optimization technique

Genetic Algorithms (GAs) are adaptive heuristic search algorithm premised on the evolutionary ideas of natural selection and genetic. The basic concept of GAs is designed to simulate processes in natural system necessary for evolution, specifically those that follow the principles first laid down by Charles Darwin of survival of the fittest. As such they represent an intelligent exploitation of a random search within a defined search space to solve a problem. Genetic Algorithms has been widely studied, experimented and applied in many fields in engineering worlds. Not only does GAs provide alternative methods to solving problem, it consistently outperforms other traditional methods in most of the problems link. Many of the real world problems involved finding optimal parameters, which might prove difficult for traditional methods but ideal for GAs. A solution for a given problem is represented in the form of a string, called "chromosome", consisting of a set of elements, called "genes", that hold a set of values for the optimization variables (the decision variables). The fitness of each chromosome is determined by evaluating it against an objective function. The chromosome represents a feasible solution for the problem under study. The length of the chromosome equals the number of variables. A Gene value is real coding (actual values). The concept of GA is based on the initial selection of a relatively small population. Each individual in the population represents a possible solution in the parameter space. The fitness of each individual is determined by the value of the objective function, calculated from a set of parameters. The natural evolutional processes of reproduction, selection, crossover, and mutation are applied using probability rules to evolve the new and better generations. The probabilistic rules allow some less fit individuals to survive. The objective of this study is to

HESSD
11, 11395–11438, 2014

maximize the benefit function Z with respect to pumping rate to obtain optimal location of wells, Q_j as design variable.

$$\max Z = \sum_{j=1}^{N_w} Q_j - P_j \tag{2}$$

in which: N_w is the total number of pumping wells and P_j is penalty.

The management objectives must be achieved within a set of constraints. The constraints may be decision variables. The objective function are subject to the following constrains:

1. pumping constraint, the pumping rates at potential pumping wells in the water demand were constrained to values between some minimum (Q_j^{min}) and maximum (Q_j^{max}) permissible pumping rates as the following:

   $$Q_j^{min} \le Q_j \le Q_j^{max} \quad j = \ldots, N_w \tag{3}$$

   In the GA simulation, this constraint can be easily satisfied by restricting the population space of the design variables to be within the above limits. Hence, no special treatment is needed for this constraint.

2. drawdown constraint, this constraint normally meant to protect the ecosystem by avoiding excessive drawdown. In this work, the drawdown constraints were formulated to avoid mining and formulated as follows:

   $$\sum_{j=1}^{N_w} r_j \le d_i \tag{4}$$

   in which: r_j is the drawdown at control point i caused by a pumping rate from pumping well j, d_i is the permissible drawdown at control point i.

HESSD
11, 11395–11438, 2014

3. water demand constraint, the Nubian sandstone aquifer was considered as the sole source of water. This, therefore, means that the designed optimal pumping strategy must supply at least the minimum water demand. It was formulated as follows:

$$\sum_{j=1}^{N_w} Q_j \geq Q_D \tag{5}$$

in which: Q_D is water demand.

4. distance between wells constraint;

$$D_i \geq D_{all} \tag{6}$$

Where D_i is actual distance between wells and D_{all} is minimum distance between wells.

5. location of wells; the locations of wells constraint is to be decided by the model itself within a user defined region of the model grid until the optimal location is reached (Fig. 6).

2.5.1 Optimization procedure of the Simulation–Optimization model

In groundwater management problems, there are two sets of variables, decision variables and state variables, where the decision variable is the pumping and injection rates of wells. Also other decision variables include well locations and the on/off status of a well. By optimization techniques the decision variables can be managed to identify the best combination of them. Hydraulic head is the state variable, which is the dependent variable in the groundwater flow equation. The simulation model updates the state variables, and the optimization model determines the optimal values for all decision variables. This process is carried out in a coupled simulation-optimization model.

HESSD
11, 11395–11438, 2014

In this work, a groundwater resources management model is proposed the solution performed through a linked simulation-optimization model. MODFLOW FORTRAN code is used as the simulation of groundwater flow. This model is linked with genetic algorithm optimization. The flowchart for simulation-optimization model where FORTRAN program used to link between the simulation code and genetic algorithm is given in (Fig. 7).

2.6 Testing scenarios

After completing the stage of calibration, the output of the first round is used to replace the initial condition with the condition of implementing the exploitation policies. The testing scenarios include three proposed optimal pumping rates and well locations policies. The first scenario estimates the optimal pumping rates from 68 productive wells with their present locations. The second scenario studies the optimal locations for these 68 productive wells and their optimal pumping rates. The third one proposes water exploitation policy aimed at increasing the present productive wells by 14 wells, as a result of the increase in reclamation activities, and delineates the optimal locations of these new wells and keeping the present locations of the other 68 present wells besides estimating the optimal pumping rates for all.

3 Results and discussions

The performed steady state calibration permits the adjustment of the hydraulic conductivity, where NSATA storage changes are not significant. Thus, dynamic stress and storage effects are excluded. The relation between the calculated and observed heads is checked from the calculated-observed head curve and the variance appears as 45.966 % (Fig. 8a). This large value indicates great difference between the heads calculated by the model and actually measured heads. So, the calibration process is very important to minimize this variance to the lower possible value. After many times of changing the k values, the variance between the observed and calculated heads is minimized to 3.61 % and the calculated head values is very closely related to the field-measured head values (Fig. 8a). Based on the calibrated model, the estimated hydraulic conductivity values are ranging from 4.33 to 7.60 m day^{-1}. These values are generally more slightly than the values calculated from the field data. The difference may relate to the benchmarks, uncertainty and grid refinement.

The groundwater equipotential contour maps of NSATA during 2008 (El-Sabri et al., 2010) and during May 2010 (Aggour et al., 2012) show relatively decline in the measured groundwater level between 0.5 and 3 m within the interval from 2008 to 2010. This relatively wide decline may attribute to the intensive irrigation activities with hydraulic stresses in the NSATA.

Moreover, after performing the steady state calibration of the constructed numerical model, unsteady state calibration is undertaken to calibrate the NSATA storage. Generally, specific storage for any aquifer is the main parameter that is changed during the transient calibration. In the process of calibration of transient state, specific yield values are modified on a trial and errors basis, until a good match between the observed heads in the years 2002 and 2012 (sited in Kim and Sultan, 2002; Aggour et al., 2012) and the calculated heads are achieved. The range of the resulted specific yield after the final calibration of the transient state is found to be varying from 0.14 to 0.34 (Fig. 8b). It can be seen that, in general, there is a good agreement between the observed and simulated head values.

In addition, applying the constructed OLGA model for solving the optimization problems related to the optimal pumping rates and the optimal well locations, the initial pumping rates are assigned to each well as less than 1000 m^3 day^{-1} and more than 700 m^3 day^{-1} and then the optimization procedure explained before is used. The GA parameters used in the optimization problem are given in (Table 3). The optimal well location and pumping rate are determined, based on OLGA model, from one feasible solution to the other according to the calculated residual errors values where they

HESSD
11, 11395–11438, 2014

Title Page
Abstract Introduction
Conclusions References
Tables Figures
◀◀ ▶▶
◀ ▶
Back Close
Full Screen / Esc
Printer-friendly Version
Interactive Discussion

improve quickly in the early iterations and change slowly in subsequent iterations till satisfying the constraints.

On the other side, the results of the three testing optimal policies applying OLGA model show the future predictions in the optimal pumping rates after 5, 10, 15, 20, 25, 30, 40 and 50 years. The first scenario investigates the optimal pumping rates from the 68 productive wells penetrating the NSATA under their current locations. The OLGA simulation results show that the optimal pumping rates, under the present conditions, range from 57 584.6 to 50 144.4 $m^3 day^{-1}$ with corresponding total drawdown ranges from 3.42 to 13.73 m during the simulation period of 50 years (Table 4).

Moreover, by running the developed OLGA model for time step of 5 years, the predicted head distribution maps of the NSATA under the current pumping rates at years 2015, 2025, 2035 and 2060 are shown in (Fig. 9). It is noticed from (Fig. 9) that the groundwater levels change from 164.5 to 161.3 m a.s.l. in the center of the cone of depression. Few productive wells in the southwestern part of the model domain show relatively slight drawdown amounts to 13 m at East El-Emaratiah Company well field. This is mainly attributed to the effect of increasing the thickness of water bearing formation towards the northwestern and western parts. In addition, one large cone of depression will develop in the cultivated areas. This cone is in the central part of Abu Simple-Tushki road and may attribute to the present extraction rates from the reclaimed areas.

Otherwise, the second scenario seems to be theoretical more than practical since it studies the optimal locations of already 68 drilled productive wells and their optimal pumping rates. The GA parameters used in this optimization case are given in (Table 5). The initial pumping rates are assigned to each well as less than 1500 $m^3 day^{-1}$ and the optimal pumping rates after 5, 10, 15, 20, 25, 30, 40 and 50 years are predicted (Table 5). It is noticed from (Table 5) that the number of the total operating wells N is still constant (68 wells), and the maximum drawdown (r) ranges from 2.22 to 12.13 m while Q_{min}/well begins with 1460.6 and ends by 1053.2 $m^3 day^{-1}$ for the simulation

HESSD
11, 11395–11438, 2014

period. The total optimal pumping rate for all wells (Q_{opt}) ranges between 102 037.6 and 100 773.3 $m^3\,day^{-1}$ (Table 5).

In the same side, the results of the OLGA model based on this scenario show that the predicted optimal location of the productive wells differ more or less from the present location (Fig. 10). Although the proposed OLGA approach successfully identified all the well locations and pumping rates of the present numerical study, identification of all the well locations and pumping rates may not be feasible for real-world applications since the number of pumping wells is usually very high. Instead, the proposed procedure may be applied to the suspected illegal pumping areas as noticed in the field trips. As an extension of this study, the performance of the proposed OLGA model should be tested on a real field system in a future study.

Otherwise, the predicted head distribution maps of the NSATA under the 2nd scenario (Fig. 11) show groundwater levels change from 165.5 to 162.5 m a.s.l. in the center of the cone of depression. It is noticed from (Fig. 11) that the normal decline in the groundwater levels (3 m) may attribute to the small thickness and low hydraulic conductivity of the NSATA in these localities. Moreover, the cone of depression will appear in the cultivated areas during the simulation time (with diameter of 2.5 to 4 km approximately). While the southern and western cultivated parts of the model domain does not be affected with this scenario. This may attribute to the effect of the great aquifer thickness and the presence of thin clay layers in the southern and western parts rather than the geologic structure impact. Accordingly, this reflects the low potentiality of the northern cultivated parts for positive response to this scenario.

The third scenario proposes water exploitation policy aimed at increasing the present productive wells by 14 wells, as a result of the increase in reclamation activities, and delineates the optimal locations of these new productive wells and keeping the present locations of the other 68 present productive wells besides estimating the optimal pumping rates for all. The GA parameters used in this optimization case are given in (Table 6). The OLGA model was run for time step of 5 years. The predicted optimal location of the new productive wells is checked (Fig. 12) and the predicted head distribution maps

HESSD
11, 11395–11438, 2014

of the NSATA for the optimal pumping rates at years 2015, 2025, 2035 and 2060 are shown in (Fig. 13).

It is noticed from (Table 5) that the number of the total operating wells N is increased to 82 productive wells, and the maximum drawdown r ranges from 4.27 to 14.56 m while Q_{min}/well begins with 923.2 and ends by 800 m^3 day^{-1} during the simulation period. The total optimal pumping rate for all wells (Q_{opt}) ranges between 87 186.7 and 79 746.5 m^3 day^{-1} (Table 6).

However, it is noticed from the predicted head distribution maps (Fig. 13) that the groundwater level decreases from 163 m a.s.l. in the beginning of the simulation period (the year 2015) to 158 m a.s.l. in the end of the simulation period (the year 2060). The depression cones related to the first and the second scenarios are mitigated in the northern part of the model domain. Moreover, limits are placed on the total optimal pumping rates of the productive groundwater wells beside its optimal locations in the reclaimed areas. Accordingly, it is preferred to extend the future reclamation activities parallel to the western side of the Khour Tushki area. Although the results of this scenario provide more or less good degree of confidence in the optimal location of the new productive wells and optimal pumping rates, the expected sharp decline in groundwater levels in the concerned area assumes more applied studies. As a result of the above discussion of the OLGA simulation results of the optimal well location and pumping rates, it can be concluded that the groundwater withdrawal from the NSATA under this optimization study could be safely conducted.

4 Conclusions and recommendations

The purpose of this study is to possible enhancements for well placement optimization with GAs. The main contributions of this work are:

A computer programming with FORTRAN language has been originally established to apply the principles of the genetic algorithm for studying the optimal location of the groundwater productive wells as a principal tool for groundwater resources

HESSD
11, 11395–11438, 2014

S. Khalaf and M. I. Gad

management. The Optimal Location applying Genetic Algorithm (OLGA model) links MODFLOW with genetic algorithm technique to establish a simulation optimization groundwater model. OLGA model is applied for NSATA to develop the optimal location of the groundwater productive wells with maximum pumping rate The performance of the proposed OLGA model, when applied to NSATA, under the available data, establishes its potential applicability to solve the complex groundwater management problems. Moreover, the results of the calibrated model indicate that the hydraulic conductivity of the NSATA ranges from 4.33 to 7.60 m day^{-1} and the corresponding specific yield values range from 0.14 to 0.34. Three scenarios are tested to choose the proper water exploitation policy. For the first scenario, the predicted groundwater drawdown after simulation period of 50 years ranges from 3.42 to 13.73 m while the corresponding optimal pumping rates range from 57 584.6 to 50 144.4 m^3 day^{-1}. Under the second proposed scenario, the predicted drawdown (r) and the corresponding total optimal pumping rate for all wells (Q_{opt}) ranges from 2.22 to 12.13 m and between 102 037.6 and 100 773.3 m^3 day^{-1} respectively. Moreover, based on the third proposed scenario of optimal 14 new well locations, the predicted value of (r) ranges from 4.27 to 14.56 m during the same simulation period. The predicted value of (r) based on the 3rd scenario is more or less similar to the results of the other two scenarios although the number of the operating wells is increased by 20 %. This reflects the great importance to apply the optimal well location concept in any new reclamation projects.

Based on the results of the OLGA model, it is highly recommended to choose the new productive well locations in staggered system parallel to the western side of the Khour Tushki area. The continuous monitoring of groundwater level in the study area through well distributed observation wells is recommended to update the model results and to preserve the Tushki National Project from deterioration. Also, more applied studies are needed for verification the results of this optimal well location model.

References

Aggour, T. A., Korany, E. A., Mosaad, S., and Kehew, A.: Geological conditions and characteristics of the Nubia Sandstone aquifer system and their hydrogeological impacts, Tushka area, south Western Desert, Egypt. Egy. J. PureAppl. Sci., 2012, 27–37, 2012.

Ahlfeld, D. P., Mulvey, J. M., Pinder, G. F., and Wood, E. F.: Contaminated groundwater remediation design using simulation, optimization, and sensitivity theory, 1. Model development, Water Resour. Res., 24, 431–441, 1988.

Aly, A. I. M., Froehlich, K., Nada, A., Hamza, M., and Salem, W. M.: Study of environmental isotope distribution in the Aswan High Dam Lake (Egypt) for estimating the evaporation of lake water and its recharge to adjacent groundwater, Environ. Geochem. Hlth., 15, 37–49, 1993.

Aral, M. M., Guan, J. B., and Maslia, M. L.: Identification of contaminant source location and release history in aquifers, J. Hydrol. Eng., 6, 225–234, 2001.

Ayvaz, M. T.: Identification of Pumping Well Characteristics in a Heterogeneous Aquifer System Using a Genetic Algorithm Approach, Ph.D. thesis, Department of Civil Engineering, Pamukkale University, Denizli, Turkey, 2008 (in Turkish).

Bear, J.: Hydraulics of Groundwater, McGraw-Hill, New York, 569 pp., 1979.

Chang, L. C., Chu, H. J., and Hsiao, C. T.: Optimal planning of a dynamic pump-treat-inject groundwater remediation system, J. Hydrol., 342, 295–304, 2007.

CONOCO: Geological Map of Egypt, NF 36 NW El Sad El-Ali, Scale 1 : 500 000, The Egyptian General Petroleum Corporation, Conoco Coral, 1987.

Desert Research Center (DRC): Evaluation of crop unit in El wadi El Gadid district, unpublished internal report, submitted, MWRI – Desert Research Center, 112 pp., 2005.

El-Sabry, M. A. S., El-Sheikh, A. E., and El-Osta, M. M.: The hydrogeological connection between Lake Nasser and the Nubian Sandstone aquifer in Tushka area, South Western Desert, Egypt, Egypt. J. Aqua. Res., 36, 245–262, 2010.

El-Shazly, E. M., Abdel Hady, M. A., El Ghawaby, M. A., Soliman, A. B., El-Kassas, I. A., Khawaski, S. M., El Amin, H., El Rakaiby, M. M., El Aasy, I. E., Abdel Megid, A. A., and Mansour, S. I.: The Geologic Map of Egypt, the Structural Lineation Map of Egypt, and the Drainage Map of Egypt Based on LANDSAT-1 Imagery Interpretation and Field Investigations, 12 maps, scale 1 : 100 000, Remote Sensing Center, Oklahama and United Nations

Environment Program (GEMS), Academy of Scientific Research and Technology, Cairo, Oklahama state University, Stillwater, 1980.
Ferreira da Silva, J. and Haie, N.: Optimal locations of groundwater extractions in coastal aquifers, Water Resour. Manag., 21, 1299–1311, 2007.
Gad, M. I. and Khalaf. S.: Application of sharing genetic algorithm for optimization of groundwater management problems in Wadi El-Farigh, Egypt, J. Appl. Water Sci., 3, 701–716, 2013.
Gad, M. I., El-Sheikh, A., and El-Osta. M. M.: Optimal management for groundwater of Nubian aquifer in El-Dakhla depression, Western Desert, Egypt, J. Water Resour. Environ. Eng., 3, 393–409, 2011.
Gorelick, S. M.: A review of distributed parameter groundwater management modeling methods, Water Resour. Res., 19, 305–319, 1983.
Guan, J. and Aral, M. M.: Optimal remediation with well locations and pumping rates selected as continuous decision variables, J. Hydrol., 221, 20–42, 1999.
Guan, J., Kentel, E., and Aral, M. M.: Genetic algorithm for constrained optimization models and its application in groundwater resources management, J. Water Res. Pl.-ASCE, 134, 64–72, 2008.
Gulver, T. B. and Shoemaker, C. A.: Dynamic optimal control for groundwater remediation with flexible management periods, Water Resour. Res., 28, 629–641, 1992.
Hamid, R. S., Fatemeh, D., and Miguel, A. M.: Simulation–Optimization Modeling of Conjunctive Use of Surface Water and Groundwater, Water Resour. Manag., 24, 1965–1988, doi:10.1007/s11269-009-9533-z, 2009.
Huang, C. and Mayer, A. S.: Pump-and-treat optimization using well locations and pumping rates as decision variables, Water Resour. Res., 33, 1001–1012, 1997.
Kim, J. and Sultan, M.: Assessment of the long-term hydrologic impacts of Lake Nasser and related irrigation projects in southwestern Egypt, J. Hydrol., 262, 68–83, 2002.
Korany, E. A., Aggour, T. A., Mosaad, S., Kehew, A., and Salim, A. A.: Hydrogeological impacts of recent recharge to Nubia sandstone aquifer in Tushka-Abu Simble area, Western Desert, Egypt, Egy. Jour. Geol., 56, 33–51, 2012.
Liu, Q., Zou, L., and Li, H.: The application of genetic algorithms in groundwater management, World Geol., 21, 145–149, 2002.
Mahar, P. S. and Datta, B.: Identification of pollution sources in transient groundwater systems, Water Resour. Manage., 14, 209–227, 2000.

HESSD
11, 11395–11438, 2014

Optimal well locations using genetic algorithm for Tushki Project

S. Khalaf and M. I. Gad

Mahar, P. S. and Datta, B.: Optimal identification of ground-water pollution sources and parameter estimation, J. Water Res. Pl.-ASCE, 127, 20–29, 2001.
Mantoglou, A. and Kourakos, G.: Optimal groundwater remediation under uncertainty using multi-objective optimization, Water Resour. Manag., 21, 835–847, 2007.
Mckinney, D. C. and Lin, M.: Genetic algorithm solution of groundwater management models, Water Resour. Res., 30, 1897–1906, 1994.
Moharram, S. H., Gad, M. I., Saafan, T. A., and Khalaf, S.: Optimal Groundwater Management Using Genetic Algorithm in El-Farafra Oasis, Western Desert, Egypt, Water Resour. Manag., 26, 927–948, doi:10.1007/s11269-011-9865-3, 2012.
Park, C. H. and Aral, M. M.: Multi-objective optimization of pumping rates and well placement in coastal aquifers, J. Hydrol., 290, 80–99, 2004.
Rana, T., Khan, S., and Rahimi, M.: Spatio-temporal optimization of agricultural drainage using groundwater models and genetic algorithms: an example from the Murray Irrigation Area, Australia, Hydrogeol. J., 16, 1145–1157, 2008.
Rizzo, D. M. and Dougherty, D. E.: Design optimization for multiple management period groundwater remediation, Water Resour. Res., 32, 2549–2561, 1996.
Ruperti, N. J.: Estimation of the Release History of a Contaminant Source in 2-D Groundwater Systems, in: Fourth International Conference on Inverse Problems in Engineering, Rio de Janeiro, Brazil, 317–324, 2002.
Saafan, T. A., Moharram, S. H., Gad, M. I., and Khalaf, S.: A multi-objective optimization approach to groundwater management using genetic algorithm, J. Water Resour. Environ. Eng., 3, 139–149, 2011.
Saffi, M. and Cheddadi, A.: Explicit algebraic influence coefficients: a one-dimensional transient aquifer model, Hydrolog. Sci. J., 52, 763–776, 2007.
Singh, R. M., Datta, B., and Jain, A.: Identification of unknown groundwater pollution sources using artificial neural networks, J. Water Res. Pl.-ASCE, 130, 506–514, 2004.
Sultan, M., Sturchio, N., Hassan, F. A., Hamdan, M. A. R., Ahmood, A. M., El Alfy, Z., and Stein, T.: Precipitation source inferred from stable isotopic composition of Pleistocene groundwater and carbonate deposits in the Western Desert of Egypt, Quaternary Geol., 4, 29–37, 1997.
Sultan, M., Yan, E., Ballerstein, E., and Becker, R.: Hydrologic impacts of Lake Nasser and the Tushka lakes on the Nubian aquifer in SW Egypt, Geological Society of America Annual Meeting Abstracts with Programs Vol. 35, No. 6, p. 198, September 2003.

HESSD
11, 11395–11438, 2014

Optimal well locations using genetic algorithm for Tushki Project

S. Khalaf and M. I. Gad

Sun, A. Y., Painter, S. L., and Wittmeyer, G. W.: A robust approach for iterative contaminant source location and release history recovery, J. Contam. Hydrol., 88, 181–196, 2006.
Tung, C. P. and Chou, C. A.: Pattern classification using tabu search to identify the spatial distribution of groundwater pumping, Hydrogeol. J., 12, 488–496, 2004.
Wang, W. and Ahlfeld, D. P.: Optimal groundwater remediation with well location as a decision variable – model development, Water Resour. Res., 30, 1605–1618, 1994.
Wanger, B. J. and Gorelick, S. M.: Reliable aquifer remediation in the presence of spatially variable hydraulic conductivity: from data to design, Water Resour. Res., 25, 2211–2225, 1989.
Yan, T., Wu, J., and Xue, Y.: A comparison of genetic algorithm and trial-and-error approach in solving the hydrogeologic inverse problem, in: Proceedings of the international Symposium on Water Resources and the Urban Environment, China Environment Science Press, Beijing, 9–10 November, 137–141, 2003.
Yao, L., Li, J., and Li, Z.: Parameter identification of groundwater flow numerical modeling by means of improved genetic algorithm, J. Hydraul. Eng.-ASCE, 34, 40–46, 2003.
Zheng, C. M. and Wang, P. P.: An integrated global and local optimization approach for remediation system design, Water Resour. Res., 35, 137–148, 1999.
Zhu, X., Wu, J., Ye, S., Zhao, J., and Wu, M.: Evaluation of groundwater resource in deep aquifers of the Yangtze Delta (south of the Yangtze Delta), in: Proceedings of the international Symposium on Water Resources and the Urban Environment, China Environment Science Press, Beijing, 9–10 November, 467–473, 2003.

HESSD
11, 11395–11438, 2014

Optimal well locations using genetic algorithm for Tushki Project

S. Khalaf and M. I. Gad

Table 1. Results of step drawdown test analysis in NSATA.

Step No.	Step time (hour) Duration (hour)	Well discharge Q ($m^3\,day^{-1}$)	Total DD (s) (m)	s/Q ($day\,m^{-2}$)
I	1.5	1080	8.32	0.008666667
II	1.5	1200	11.8	0.009833333
III	1.5	1368	13.38	0.009291667
IV	1.5	1488	15.82	0.01063172

HESSD
11, 11395–11438, 2014

Table 2. Results of long duration pumping tests analysis in NSATA.

Well No.	Well coordinates		Total	Static water	Total
	Longitude	Latitude	depth (m)	level (m)	DD (m)
W 85	31°31′03″ E	22°28′2.5″ N	199	58.2	11.25
W 9′	31°38′46″ E	22°43′25″ N	200	41.41	8.63
W11	31°38′10″ E	22°41′10″ N	199.5	46.38	6.68
Well Kilo zero	31°51′04″ E	22°38′03″ N	34.5	21.3	8.3
Recharge well	31°42′33″ E	22°22′33″ N	184.5	20.88	15.39

HESSD
11, 11395–11438, 2014

Table 3. The GA solution parameters applying OLGA model.

Continuous GA Parameter	Value
Population size	200
Mutation ratio	0.006
Type of crossover	uniform crossover
Crossover probability	0.7
Tolerance for the convergence of iterations	0.01

HESSD
11, 11395–11438, 2014

S. Khalaf and M. I. Gad

Table 4. Optimal pumping rate for first scenario.

Year	5	10	15	20	25	30	40	50
N	68	68	68	68	68	68	68	68
r (m)	3.42	5.62	6.78	7.88	8.93	9.96	11.85	13.73
Q_{min}/well	746.8	726.4	708.6	695.6	645.2	629.2	613.8	605.7
Q_{max}/well	1000	1000	1000	1000	1000	1000	1000	1000
Q_{opt} (m^3 day^{-1})	57 584.6	56 032.8	54 511.4	53 021.2	52 291.6	51 568.4	50 852.3	50 144.4

N is number of operation wells, r is maximum drawdown, Q_{min}/well is min optimal pumping rate for well, Q_{max}/well is max optimal pumping rate for well and Q_{opt} total optimal pumping rate for all wells.

HESSD
11, 11395–11438, 2014

Table 5. Optimal pumping rate for the 2nd scenario applying OLGA model.

Year	5	10	15	20	25	30	40	50
N	68	68	68	68	68	68	68	68
r (m)	2.22	4.32	5.43	6.63	7.73	8.64	10.53	12.13
Q_{min}/well	1460.6	1369.5	1301.6	1286.4	1201.3	1183.2	1102.4	1053.2
Q_{max}/well	1500	1500	1500	1500	1500	1500	1500	1500
Q_{opt} (m^3 day^{-1})	102 038	101 797	101 561	101 330	101 103	100 992	100 882	100 773

Discussion Paper | Discussion Paper | Discussion Paper | Discussion Paper |

HESSD

11, 11395–11438, 2014

Optimal well locations using genetic algorithm for Tushki Project

S. Khalaf and M. I. Gad

Table 6. Optimal pumping rate for third scenario.

Year	5	10	15	20	25	30	40	50
N	82	82	82	82	82	82	82	82
r (m)	4.27	6.47	7.63	8.72	9.77	10.80	12.68	14.56
Q_{min}/well	923.2	913.3	902.8	879.6	823.6	813.2	800	800
Q_{max}/well	1500	1500	1500	1500	1500	1500	1500	1500
Q_{opt} (m^3 day^{-1})	87 186.7	85 634.9	84 113.5	82 623.3	81 893.7	81 170.5	80 454.4	79 746.5

HESSD
11, 11395–11438, 2014

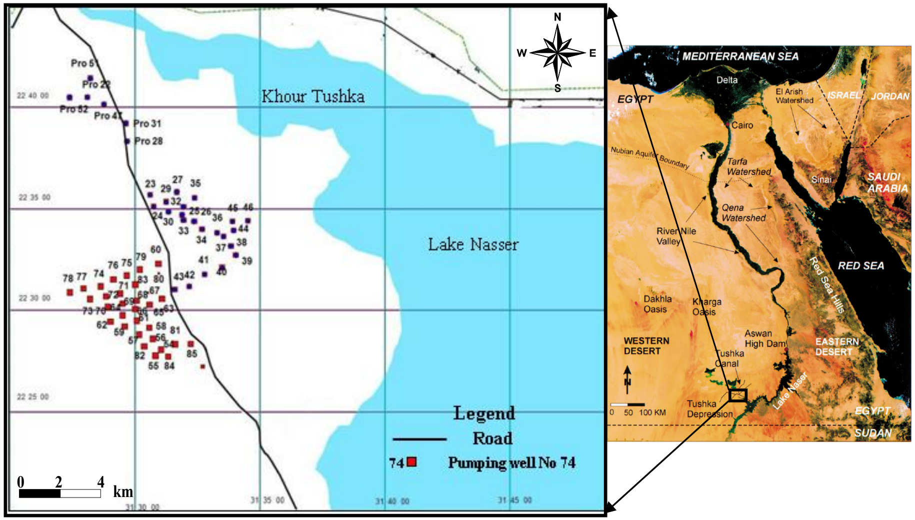

Figure 1. Location map of the study area showing the location of 48 flowing wells.

HESSD

11, 11395–11438, 2014

Optimal well locations using genetic algorithm for Tushki Project

S. Khalaf and M. I. Gad

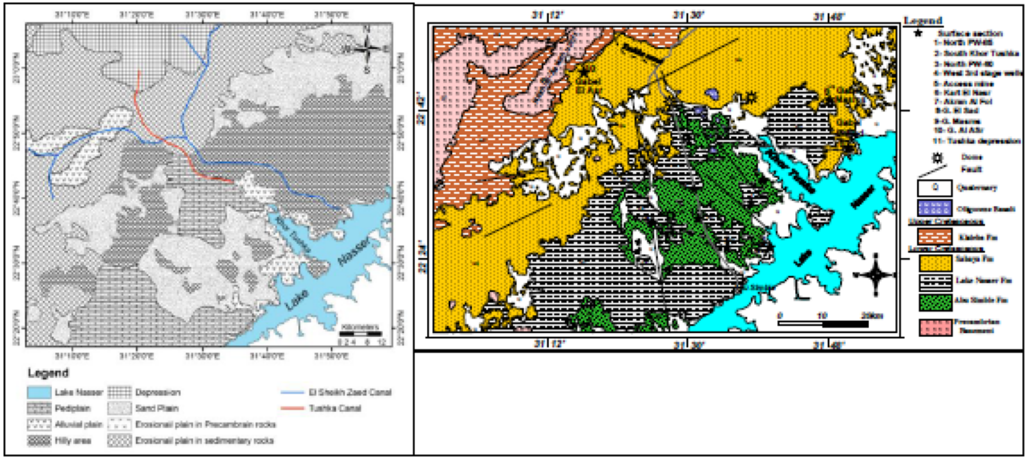

Figure 2. Constructed geomorphologic map (left map, after Aggour et al., 2012) and geological map (right map, modified after Conoco, 1987) of the study area.

HESSD
11, 11395–11438, 2014

Optimal well locations using genetic algorithm for Tushki Project

S. Khalaf and M. I. Gad

Title Page
Abstract | Introduction
Conclusions | References
Tables | Figures
◀| |▶
◀ ▶
Back | Close
Full Screen / Esc
Printer-friendly Version
Interactive Discussion

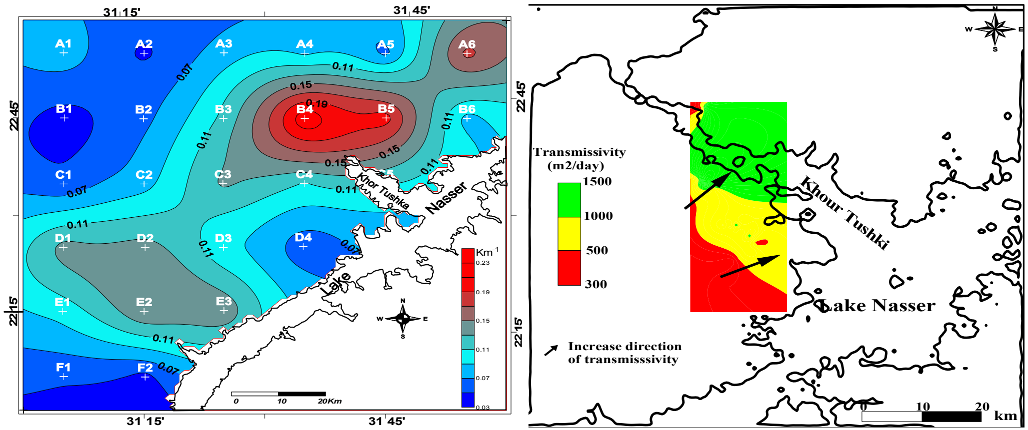

Figure 3. Density contour map of the structural lineaments (left map – after Aggour et al., 2012) and the transmissivity distribution contour map (right map) of the NSATA.

HESSD
11, 11395–11438, 2014

Optimal well locations using genetic algorithm for Tushki Project

S. Khalaf and M. I. Gad

Title Page
Abstract | Introduction
Conclusions | References
Tables | Figures
◀| |▶
◀ ▶
Back | Close
Full Screen / Esc
Printer-friendly Version
Interactive Discussion

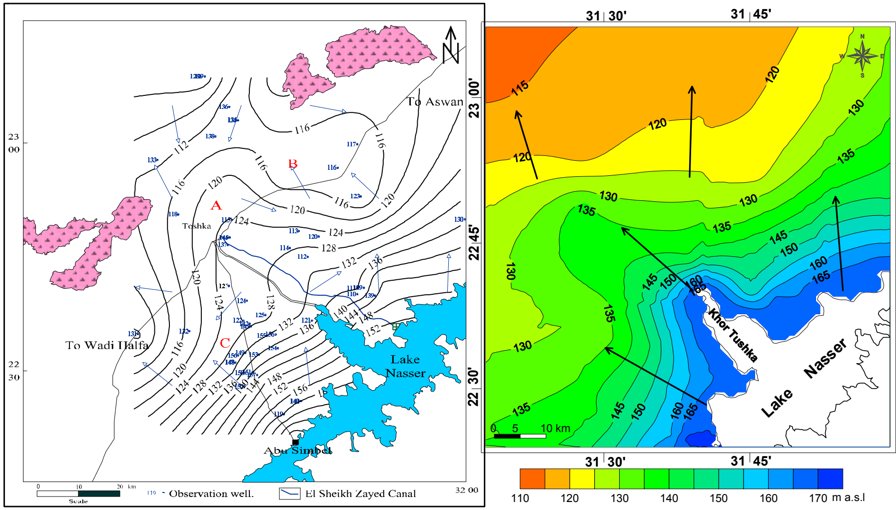

Figure 4. The groundwater equipotential and flow maps of NSATA during 2008 (left map after El-Sabri et al., 2010) and during May 2010 (right map – after Aggour et al., 2012).

HESSD
11, 11395–11438, 2014

Optimal well locations using genetic algorithm for Tushki Project

S. Khalaf and M. I. Gad

Title Page
Abstract Introduction
Conclusions References
Tables Figures
◂ ▸
Back Close
Full Screen / Esc
Printer-friendly Version
Interactive Discussion

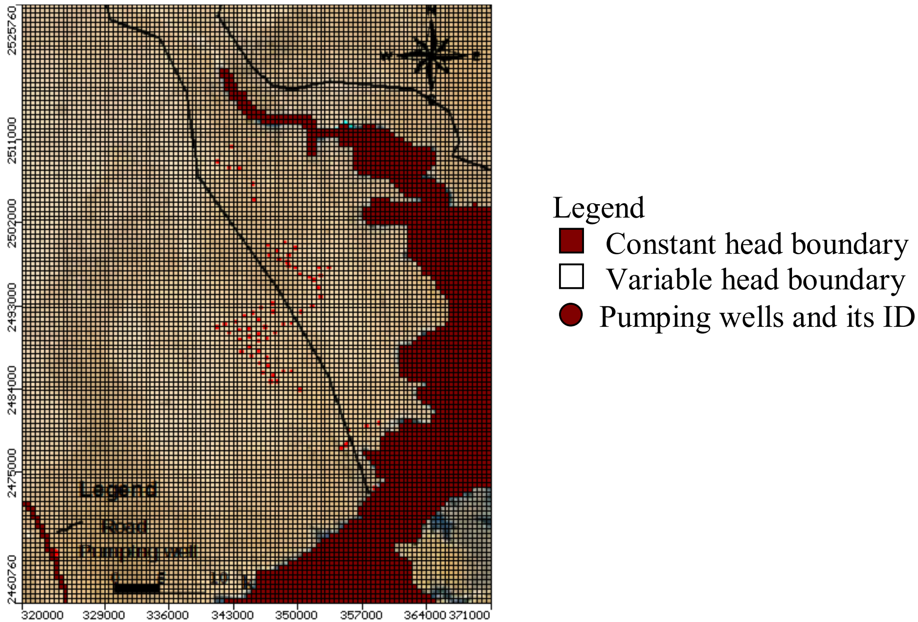

Figure 5. Flow model domain grid and the boundary conditions of the NSATA model.

HESSD
11, 11395–11438, 2014

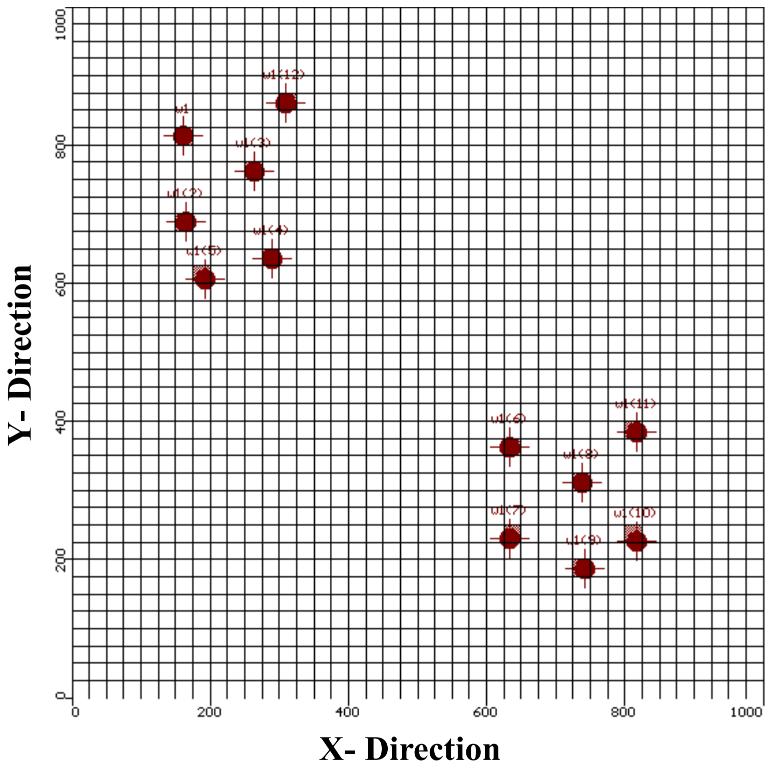

Figure 6. Plan view showing finite difference grid with sub-domain for well locations.

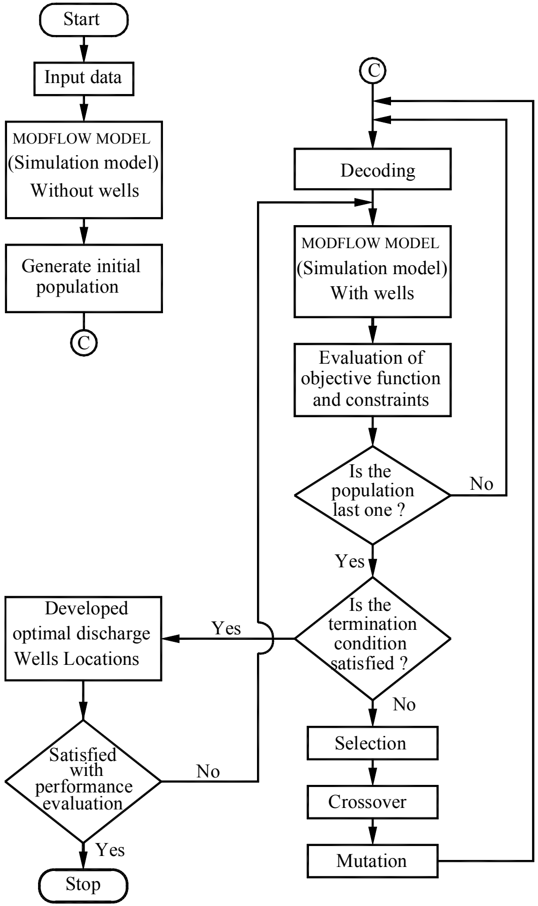

Figure 7. Flowchart for the simulation/optimization model.

HESSD
11, 11395–11438, 2014

Optimal well locations using genetic algorithm for Tushki Project

S. Khalaf and M. I. Gad

Title Page
Abstract Introduction
Conclusions References
Tables Figures
◂I ▸I
◂ ▸
Back Close
Full Screen / Esc
Printer-friendly Version
Interactive Discussion

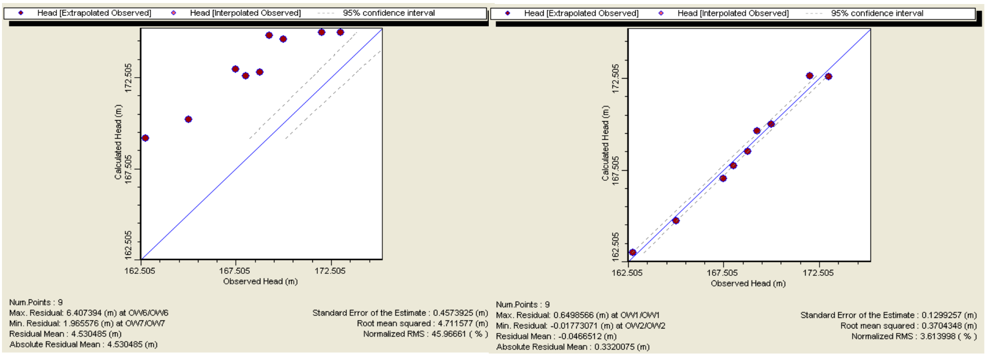

Figure 8a. The calculated and observed heads of the model domain of NSATA for steady state.

HESSD
11, 11395–11438, 2014

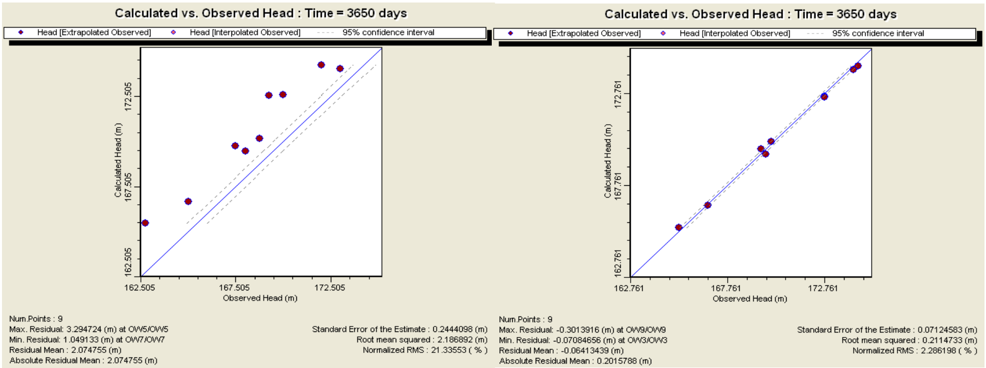

Figure 8b. The calculated and observed heads of the model domain of NSATA for unsteady.

HESSD
11, 11395–11438, 2014

Optimal well locations using genetic algorithm for Tushki Project

S. Khalaf and M. I. Gad

Title Page
Abstract | Introduction
Conclusions | References
Tables | Figures
◂| |▸
◂ ▸
Back | Close
Full Screen / Esc
Printer-friendly Version
Interactive Discussion

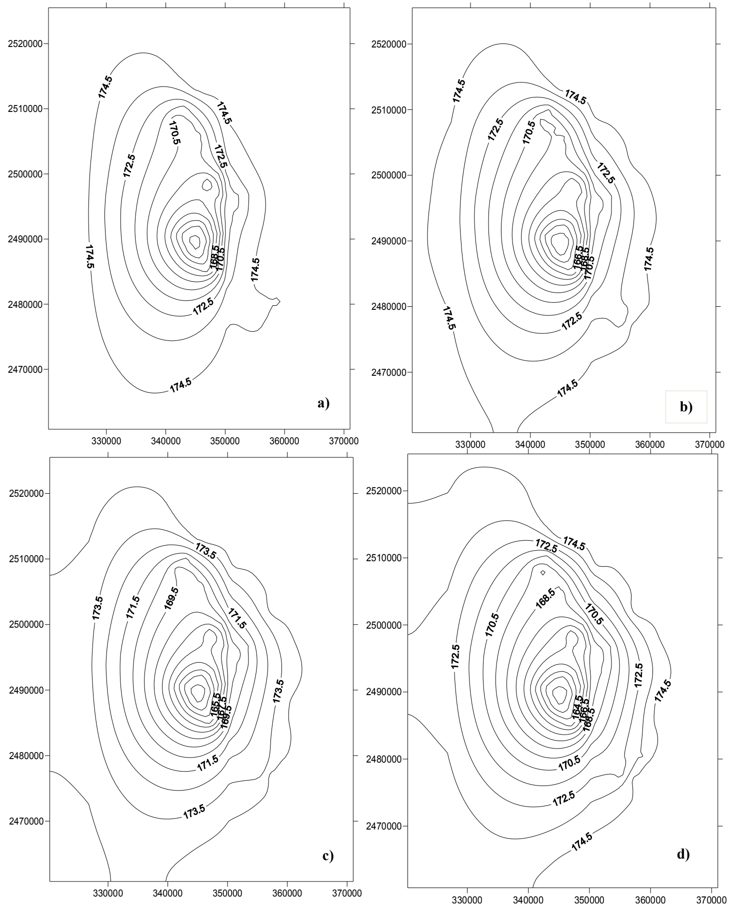

Figure 9. Predicted head distribution map of the NSATA for optimal pumping rates applying 1st scenario **(a)** at 2015, **(b)** at 2025, **(c)** at 2035, and **(d)** at 2060.

HESSD
11, 11395–11438, 2014

Title Page
Abstract | Introduction
Conclusions | References
Tables | Figures
◄| |►
◄ ►
Back | Close
Full Screen / Esc
Printer-friendly Version
Interactive Discussion

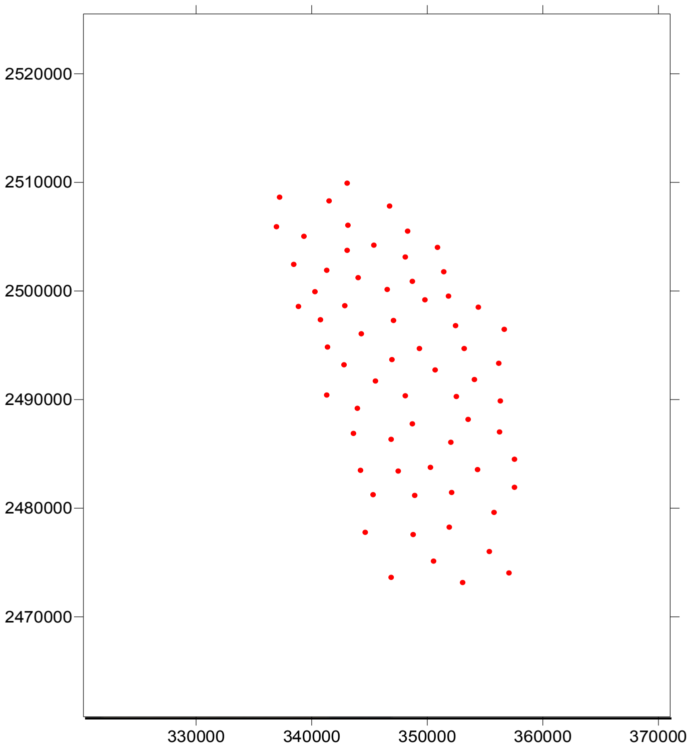

Figure 10. Optimal location of wells (2nd scenario).

Discussion Paper | Discussion Paper | Discussion Paper | Discussion Paper |

HESSD
11, 11395–11438, 2014

Optimal well locations using genetic algorithm for Tushki Project

S. Khalaf and M. I. Gad

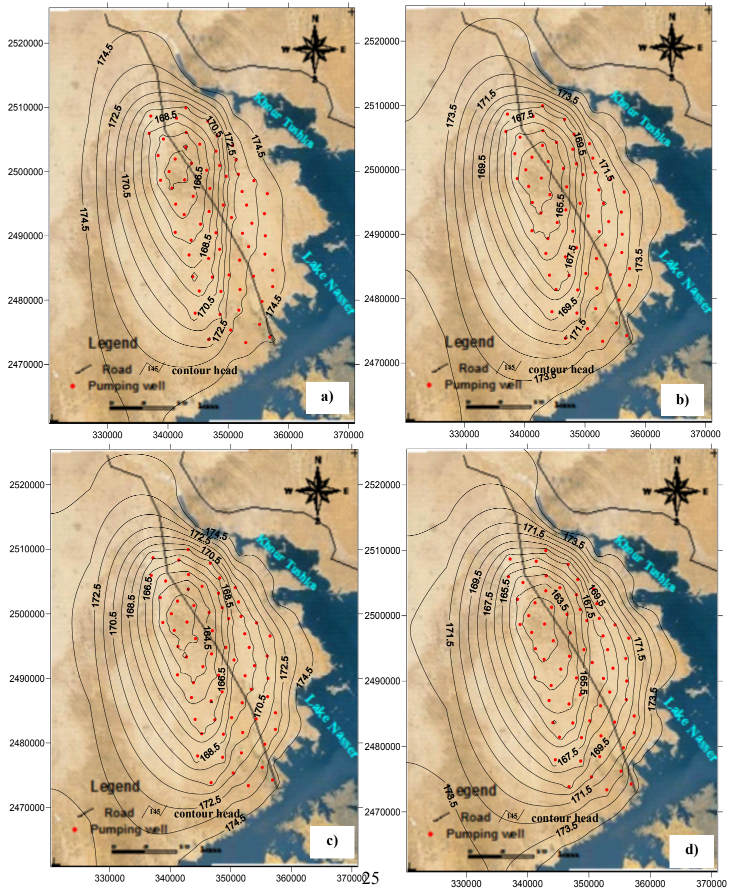

Figure 11. Predicted head distribution maps of the NSATA for optimal well locations applying 2nd scenario **(a)** at 2015, **(b)** at 2025, **(c)** at 2035, and **(d)** at 2060.

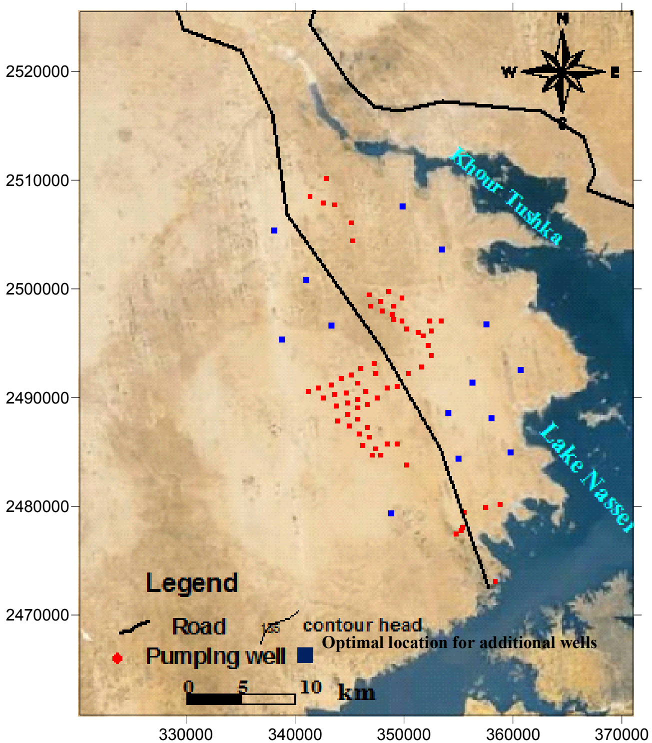

Figure 12. Optimal location of the new productive wells (3rd scenario).

HESSD
11, 11395–11438, 2014

Optimal well locations using genetic algorithm for Tushki Project

S. Khalaf and M. I. Gad

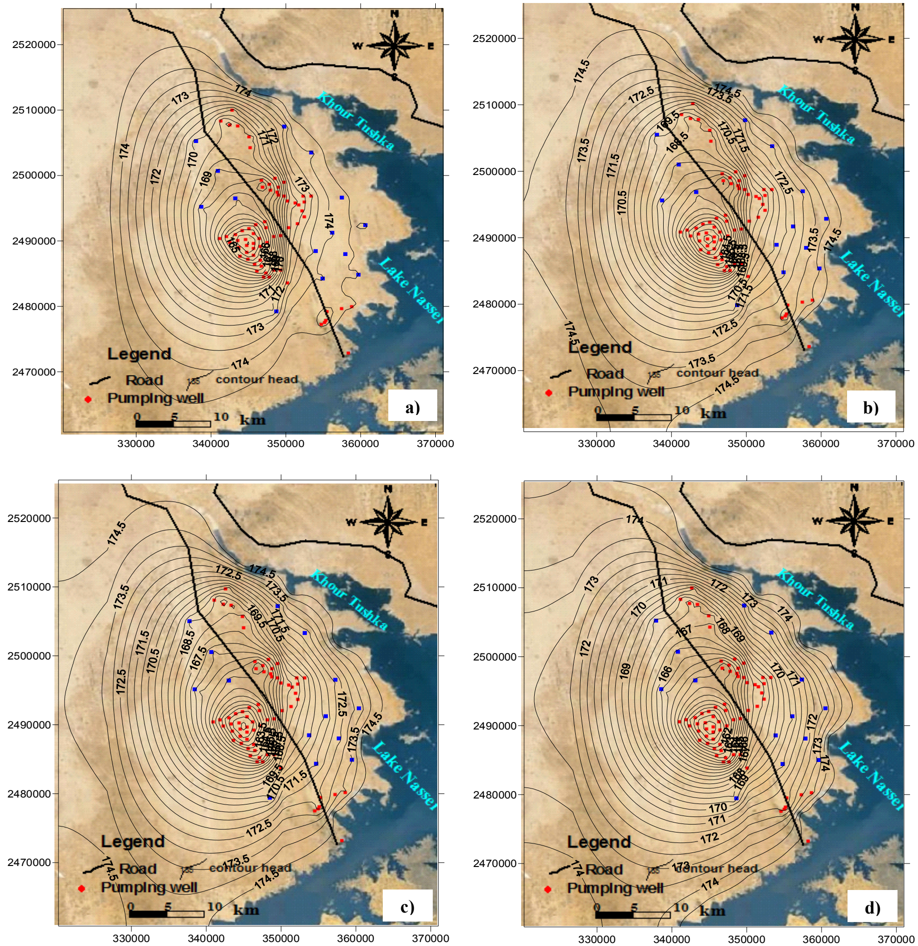

Figure 13. Predicted head distribution maps of the NSATA for optimal well locations applying 3rd scenario **(a)** at 2015, **(b)** at 2025, **(c)** at 2035, and **(d)** at 2060.

HESSD
11, 11395–11438, 2014

Optimal well locations using genetic algorithm for Tushki Project

S. Khalaf and M. I. Gad

Title Page
Abstract
Introduction
Conclusions
References
Tables
Figures
◀▏
▕▶
◀
▶
Back
Close
Full Screen / Esc
Printer-friendly Version
Interactive Discussion